NATIONAL ADVISORY COMMITTEE FOR AERONAUTICS

TECHNICAL NOTE 3077

THE EFFECT OF DYNAMIC LOADING ON THE STRENGTH OF AN INELASTIC COLUMN

By William A. Brooks, Jr., and Thomas W. Wilder, III

Langley Aeronautical Laboratory
Langley Field, Va.

Washington
March 1954

1K

NATIONAL ADVISORY COMMITTEE FOR AERONAUTICS

TECHNICAL NOTE 3077

THE EFFECT OF DYNAMIC LOADING ON THE STRENGTH OF AN INELASTIC COLUMN

By William A. Brooks, Jr., and Thomas W. Wilder, III

SUMMARY

The maximum loads of idealized inelastic H-section columns whose pinned ends approach each other at a constant rate are presented. The solutions indicate that as the rate of end displacement becomes smaller the dynamic buckling solutions approach the static solution as a lower limit. The effects of inertia forces are apparently negligible at rates of end displacement comparable to those normally used in static column tests. For all rates of end displacement investigated the static maximum load may be employed as a conservative estimate of the maximum column load.

INTRODUCTION

Only in recent years has the solution to the problem of the statically loaded inelastic column been sufficiently developed to provide answers as satisfactory as those predicted from elastic-column theory. Shanley (ref. 1) gave new life to inelastic-column theory by indicating that a column may start to bend at the tangent-modulus load and that the maximum load of a straight inelastic column is always less than the reduced-modulus load but greater than the tangent-modulus load. By extending Shanley's theory, Duberg and Wilder (ref. 2) found that the maximum load could be determined more definitely and that it depended, for a large part, on the shape of the stress-strain curve. It was later shown (ref. 3) that the maximum load of an initially curved inelastic column may be less than the tangent-modulus load, and that initial out-of-straightness has a greater effect on the maximum load of an inelastic column than on that of an elastic column.

Whereas the behavior of columns subjected to static loading conditions is comparatively well known, investigations involving the behavior of dynamically loaded columns have been limited in scope and number in spite of the fact that most structural loads, in particular the most significant aircraft structural loads, are dynamic. Hoff and his associates (refs. 4 and 5) treated the case of an elastic column whose ends

approach each other at a constant rate and showed that for rates of end displacement comparable to those obtained in static-testing machines there is good agreement between the maximum load and the Euler load. It was also shown that at higher rates the maximum load becomes greater than the Euler load. The inelastic column was analyzed in much the same manner by Chawla (ref. 6), who found that for relatively slow rates of end displacement the maximum column load was much smaller than the tangent-modulus load. Chawla's results appeared low; therefore, a static solution was made by the authors which revealed that the maximum load obtained in reference 6 was not only less than the tangent-modulus load but also less than the static maximum load. If this surprising result is correct, the consequences are indeed serious because its indication is that a static analysis could not be used to obtain a conservative estimate of the maximum load.

The present paper gives the results of an analysis which was made to ascertain whether some particular combination of the factors which influence the strength of inelastic columns would cause the strength of the column to be less when rapidly loaded than when slowly loaded. The only manner of loading which is considered is that which causes the pinned ends of the column to be axially displaced with a constant velocity. The factors considered most important for the study are the initial out-of-straightness, the shape of the stress-strain curve, the slenderness ratio of the column, and the rate at which the ends of the column are displaced. The parameters which describe these factors are varied to yield numerous solutions which show the influence of each factor on the strength of the column.

The column used in the analysis is the idealized H-section column. The analytical expression used for the stress-strain curves is that proposed by Ramberg and Osgood (ref. 7) and is assumed to be unaffected by the rate of loading.

SYMBOLS

A	cross-sectional area of column
b	column thickness (see fig. 1)
d	total lateral deflection of column at midheight after loading
d_o	initial lateral deflection of column at midheight before loading

e	dimensionless initial lateral deflection of column at midheight before loading, $2d_o/b$
E	Young's modulus
E_S	secant modulus
f	dimensionless total lateral deflection of column at midheight after loading, $2d/b$
L	column length
m	mass per unit volume of column material
n	Ramberg-Osgood stress-strain-curve shape parameter (see ref. 7)
q	lateral inertia force per unit length
t	time
v	velocity at which the ends of the column are displaced
x	longitudinal distance measured from end of column
y	total lateral deflection of column
y_o	initial lateral deflection of column
ϵ	strain
ϵ_1	elastic strain corresponding to stress σ_1
ϵ_E	elastic strain corresponding to Euler stress, $\pi^2\rho^2/L^2$
ξ	dummy variable of integration
ρ	radius of gyration, $b/2$
σ	stress
σ_1	0.7E secant yield stress
σ_T	cross-sectional stress corresponding to tangent-modulus load

$\bar{\sigma}$ average cross-sectional stress of column

τ dimensionless time parameter, $vt/L\epsilon_1$

ω first natural circular frequency in transverse bending

Ω dynamic buckling index, $\left(\frac{\omega}{v/L\epsilon_E}\right)^2$

Subscripts:

L left (concave) flange

R right (convex) flange

max maximum

rev corresponding to the strain at which reversal occurs

Dots indicate differentiation with respect to time t; primes indicate differentiation with respect to dimensionless time τ.

THEORY

The idealized pin-ended column (fig. 1) treated in the present paper consists of two thin flanges of equal area separated by a web of infinite shear stiffness and of negligible area. Inasmuch as the velocity of compression-wave propagation is large compared with both the rate of end displacement and the rate of the resulting lateral deflection, a state of uniform average compression is assumed to exist along the length of the column.

The initial conditions at time zero are

$$\left.\begin{aligned} y &= y_o \\ \dot{y} &= 0 \\ \ddot{y} &= 0 \end{aligned}\right\} \tag{1}$$

If D'Alembert's principle is applied to the portion of the column shown in figure 1, the following equilibrium equation can be obtained by summing the moments about the pin:

$$\sigma_L \frac{A}{2}\left(\frac{b}{2} - y\right) - \sigma_R \frac{A}{2}\left(\frac{b}{2} + y\right) + mA\int_0^x \ddot{y}_\xi \, d\xi = 0 \tag{2}$$

This equation relates the flange stresses σ_L and σ_R to the lateral deflection y. Another relation between the stresses and lateral deflection can be obtained through the use of the stress-strain relation of the material in conjunction with the satisfaction of compatibility between the flange strains and the lateral deflection.

In the present paper the stress-strain curve is assumed to be represented by the Ramberg-Osgood equation:

$$\frac{\epsilon}{\epsilon_1} = \frac{\sigma}{\sigma_1} + \frac{3}{7}\left(\frac{\sigma}{\sigma_1}\right)^n \tag{3}$$

This equation is used when the material is loading. Unloading (strain reversal) which may occur in the convex flange is assumed to take place elastically; thus

$$\frac{\epsilon}{\epsilon_1} = \frac{\sigma}{\sigma_1} + \frac{3}{7}\left(\frac{\sigma_{rev}}{\sigma_1}\right)^n \tag{4}$$

where σ_{rev} is the stress corresponding to the strain at which reversal occurs.

Satisfaction of compatibility requires that

$$\left.\begin{aligned} \epsilon_L &= \bar{\epsilon} - \frac{b}{2}\frac{d^2(y - y_o)}{dx^2} \\ \epsilon_R &= \bar{\epsilon} + \frac{b}{2}\frac{d^2(y - y_o)}{dx^2} \end{aligned}\right\} \tag{5}$$

where, by virtue of the assumption of uniform average compression, the average strain $\bar{\epsilon}$ is related to the end displacement as follows:

$$L\bar{\epsilon} = vt + \frac{1}{2}\int_0^L \left(\frac{dy_o}{dx}\right)^2 dx - \frac{1}{2}\int_0^L \left(\frac{dy}{dx}\right)^2 dx \tag{6}$$

By assuming the initial out-of-straightness to be

$$y_o = d_o \sin \frac{\pi x}{L} \tag{7}$$

and the total deflection to be

$$y = d \sin \frac{\pi x}{L} \tag{8}$$

and by satisfying equilibrium only at midheight $(x = L/2)$, equation (2) becomes

$$\frac{\sigma_L}{2}\left(\frac{b}{2} - d\right) - \frac{\sigma_R}{2}\left(\frac{b}{2} + d\right) + \frac{L^2}{\pi^2} m\ddot{d} = 0 \tag{9}$$

When equations (6), (7), and (8) are used, the strains (5) become

$$\left.\begin{aligned} \epsilon_L &= \frac{vt}{L} - \frac{1}{4}\frac{\pi^2}{L^2}\left(d^2 - d_o^2\right) + \frac{b}{2}\frac{\pi^2}{L^2}\left(d - d_o\right) \\ \epsilon_R &= \frac{vt}{L} - \frac{1}{4}\frac{\pi^2}{L^2}\left(d^2 - d_o^2\right) - \frac{b}{2}\frac{\pi^2}{L^2}\left(d - d_o\right) \end{aligned}\right\} \tag{10}$$

Employment of the relations

$$\epsilon_E = \frac{\pi^2}{4}\frac{b^2}{L^2}$$

$$f = 2\frac{d}{b}$$

$$e = 2\frac{d_o}{b}$$

reduces equations (9) and (10) to

$$\ddot{f} = \frac{\pi^2}{2L^2 m}\left[\sigma_L(f - 1) + \sigma_R(f + 1)\right] \tag{11}$$

and

$$\left.\begin{aligned} \epsilon_L &= \frac{vt}{L} - \frac{1}{4}\epsilon_E\left(f^2 - e^2\right) + \epsilon_E(f - e) \\ \epsilon_R &= \frac{vt}{L} - \frac{1}{4}\epsilon_E\left(f^2 - e^2\right) - \epsilon_E(f - e) \end{aligned}\right\} \tag{12}$$

The differential equation (11) can be made dimensionless by using the relation

$$\sigma_1 = E\epsilon_1 \tag{13}$$

and the parameter

$$\tau = \frac{vt}{L\epsilon_1} \tag{14}$$

A value of τ equal to unity corresponds to an end displacement sufficient to produce a strain of ϵ_1 in a straight column. Equation (11) thus becomes

$$f'' = \frac{\pi^2}{2v^2} \frac{E\epsilon_1^3}{m} \left[\frac{\sigma_L}{\sigma_1} (f - 1) + \frac{\sigma_R}{\sigma_1} (f + 1) \right] \tag{15}$$

Equations (12) are made dimensionless by dividing both sides of the equations by ϵ_1 and using equation (14):

$$\frac{\epsilon_L}{\epsilon_1} = \tau - \frac{1}{4} \frac{\epsilon_E}{\epsilon_1} \left(f^2 - e^2 \right) + \frac{\epsilon_E}{\epsilon_1} (f - e) \tag{16a}$$

$$\frac{\epsilon_R}{\epsilon_1} = \tau - \frac{1}{4} \frac{\epsilon_E}{\epsilon_1} \left(f^2 - e^2 \right) - \frac{\epsilon_E}{\epsilon_1} (f - e) \tag{16b}$$

The term before the brackets of equation (15) may be written as

$$\frac{\pi^2 E\epsilon_1^3}{2v^2 m} = \frac{\Omega}{2\left(\frac{\epsilon_E}{\epsilon_1} \right)^3} \tag{17}$$

where, by definition,

$$\Omega = \left(\frac{\omega}{v/L\epsilon_E} \right)^2 \tag{18}$$

In the expression for Ω, the quantity ω is the first natural circular frequency in transverse bending. The differential equation (15) may now be rewritten:

$$f'' = \frac{\Omega}{2\left(\epsilon_E/\epsilon_1 \right)^3} \left[\frac{\sigma_L}{\sigma_1} (f - 1) + \frac{\sigma_R}{\sigma_1} (f + 1) \right] \tag{19}$$

Simultaneous solution of equations (3) (or (3) and (4)), (16), and (19) yields the desired lateral deflection.

An additional equation which proves useful in a numerical solution is obtained by using the relation

$$\frac{\sigma}{\sigma_1} = \frac{E_S}{E}\frac{\epsilon}{\epsilon_1} \tag{20}$$

and combining equations (16) and (19) to produce

$$f'' = \frac{\Omega}{2\left(\epsilon_E/\epsilon_1\right)^3}\left\{\frac{E_{S_L}}{E}\left[\tau - \frac{1}{4}\frac{\epsilon_E}{\epsilon_1}\left(f^2 - e^2\right) + \frac{\epsilon_E}{\epsilon_1}(f - e)\right](f - 1) + \frac{E_{S_R}}{E}\left[\tau - \frac{1}{4}\frac{\epsilon_E}{\epsilon_1}\left(f^2 - e^2\right) - \frac{\epsilon_E}{\epsilon_1}(f - e)\right](f + 1)\right\} \tag{21}$$

A numerical solution of the problem is described in detail in the appendix.

RESULTS AND DISCUSSION

The cases for which solutions were obtained are given in table 1. The parameters which are varied are:

(1) The shape of the stress-strain curve, which is determined by the value of n assigned to the Ramberg-Osgood equation

(2) The slenderness ratio of the column, which is determined by the value assigned to ϵ_E/ϵ_1 (which is, in turn, defined by the value assigned to σ_T/σ_1)

(3) The initial out-of-straightness, which is determined from the value of the dimensionless parameter e

(4) The dynamic-buckling index Ω, which is inversely proportional to the square of the velocity at which the ends of the column approach each other.

An explanation of the meaning of the dynamic-buckling index Ω can be had by realizing that when a particular column is being loaded, the end displacement will reach a value equal to $\epsilon_E L$ in a time equal to that required for an identical unloaded column to undergo a natural vibration of $\sqrt{\Omega}/2\pi$ cycles. Therefore, Ω is the parameter which can be varied to correspond to various rates of end displacement. Table 2 indicates the approximate range of the velocities employed.

The dimensionless parameter τ (eq. (14)) may be considered to be a shortening parameter, as the product vt is the amount of shortening that occurs in time t. With the exception of figure 2, the results are presented as plots of load against lateral deflection or shortening.

Plots of dimensionless lateral deflection against dimensionless shortening are given in figure 2 for $n = 10$ and $e = 0.01$. The curves result from the dynamic solutions, and the symbols in this figure represent points in the neighborhood of the maximum load obtained from the static solution. At the higher velocities (small values of Ω), for a given amount of shortening, the lateral deflection is considerably smaller than that obtained from the static solution. Thus, in the dynamic solutions, more shortening initially results from axial compression than from bending, and the lateral deflections initially lag behind those obtained from the static solution. However, as time progresses it is possible for the lateral deflection obtained for all rates of end displacement to overshoot that obtained from the static solution. For $\Omega = 10^6$, the lateral deflections from the dynamic solution oscillate about those obtained from the static solution. The oscillations are so small that it is difficult and impractical to show them. For all practical purposes, the curve for $\Omega = 10^6$ coincides with that obtained from the static solution, and the effects of inertia forces are negligible.

Figure 3 presents the variation of load with lateral deflection for the cases given in figure 2. The symbols in this figure and subsequent ones represent points in the neighborhood of the maximum load obtained from the static solutions given in reference 3. It is to be noted that maximum loads are not indicated for $\Omega = 1$, 10, and 10^2. For these cases the solutions were terminated when strains became approximately equal to 2 percent. Excessive deformation rather than maximum load is believed to be the governing criterion for cases in this range of velocities.

In figure 4, load is plotted against shortening. The material stress-strain curve is also shown and, as would be expected, serves as the upper limit. However, it is important to realize that at the higher velocities the material stress-strain curve may be altered. In the present paper, the rate of end displacement is assumed to have no influence on the shape of the stress-strain curve.

In order to investigate the effect of initial out-of-straightness, a group of solutions was made for a given rate of end displacement and various values of initial curvature. The solid curves of figures 5 and 6 are these solutions and the dashed curves are the corresponding static solutions. As would be expected, the largest values of load overshoot are associated with the smallest initial out-of-straightness - a situation similar to that which exists for static loading; namely, the smallest eccentricities permit the column to bear the largest loads. However, it is apparent that initial curvatures, particularly the small out-of-straightness, have more effect on the maximum load for dynamic loading than for static loading. (The static maximum load for $e = 0$ is practically coincident with that for $e = 0.00001$.)

Figure 7 shows the results of solutions for columns of different lengths and of a given material, initial out-of-straightness, and rate of end displacement. For comparison purposes the tangent-modulus load and static maximum load are shown. The static curves were obtained from reference 3. A static curve is not given for σ_T/σ_1 $\left(\text{or } P_T/P_1\right)$ equal to 1.1 because, as a result of computational difficulties, this case was not considered in reference 3. From these plots it is evident that the tangent-modulus load may in some instances, depending on the column proportions, material, and initial out-of-straightness, be an unconservative approximation to the maximum dynamic load. For the case shown, the tangent-modulus load is a better approximation for the dynamic maximum load than for the static maximum load.

Figures 8 and 9 show solutions for a different material $(n = 2)$. A comparison of these figures with figures 3 and 4 reveals that, for a given rate of end displacement, the percentage increase in maximum load above that predicted by the static analysis is greater for the material having a more rapidly curving stress-strain curve $(n = 10)$. The load overshoot for $\Omega = 10^2$ is, in the given case, approximately 32 percent. Considering the fact that the initial out-of-straightness is rather large, it is obvious that for $n = 2$ the dynamic maximum loads for the smaller values of initial out-of-straightness may be considerably larger than the static maximum load. However, the static maximum load is still on the conservative side of the dynamic maximum load.

CONCLUDING REMARKS

The solutions presented indicate that as the rate of end displacement becomes smaller the dynamic buckling solutions approach the static solution as a lower limit. The upper limit for dynamic buckling is, as would be expected, the material stress-strain curve, which may be altered by the rate of loading. The effects of inertia forces are apparently

negligible at rates of end displacement comparable to those normally used in static column tests. From the results obtained it can be concluded that the static maximum load may be employed as a conservative estimate of the maximum load of a column, regardless of the rate of end displacement.

Langley Aeronautical Laboratory,
National Advisory Committee for Aeronautics,
Langley Field, Va., December 29, 1953.

APPENDIX

NUMERICAL SOLUTION

The nonlinear nature of the differential equation of lateral column motion makes it necessary to resort to a numerical solution. The solution is facilitated by the fact that the equation of motion does not contain the velocity of lateral deflection; only the deflection and acceleration are involved. By approximating the acceleration with an interpolation formula and integrating twice, a recursion formula for forward integration can be obtained. Once the type of integrating formula has been decided upon, it is necessary only to obtain the required initial values and to choose the interval size. In the sections that follow, each of the aforementioned items will be discussed in detail.

Recursion Formulas for Forward Integration

When f is known, the strains ϵ_L and ϵ_R can be found by substituting f and the corresponding value of τ into equations (16). The stresses σ_L and σ_R can then be determined by using the stress-strain relation (3) or relations (3) and (4). If the stresses that exist at f are known, f'' can be computed from equation (19). Equation (19) may therefore be written in functional notation as

$$f'' = g(f,\tau) \tag{A1}$$

and can be integrated by use of the following recursion formula (ref. 8):

$$f_{r+1} = 2f_r - f_{r-1} + (\Delta\tau)^2\left(f''_r + \frac{1}{12}\Delta^2 f''_{r-1}\right) \tag{A2}$$

However, as the following diagonal-difference table indicates, $\Delta^2 f''_{r-1}$ is a function of f''_{r+1} and is therefore indeterminate until f''_{r+1}, which is, in turn, dependent on f_{r+1} (eq. (A1)), has been found.

DIAGONAL-DIFFERENCE TABLE

τ	f	f"	$\Delta f"$	$\Delta^2 f"$
$(r - 2)\Delta\tau$	f_{r-2}	$f"_{r-2}$		
			$\Delta f"_{r-2}$	
$(r - 1)\Delta\tau$	f_{r-1}	$f"_{r-1}$		$\Delta^2 f"_{r-2}$
			$\Delta f"_{r-1}$	
$(r)\Delta\tau$	f_r	$f"_r$		$\Delta^2 f"_{r-1}$
			$\Delta f"_r$	
$(r + 1)\Delta\tau$	f_{r+1}	$f"_{r+1}$		

An approximate solution (ref. 8) which does not require $\Delta^2 f"_{r-1}$ is the following:

$$f_{r+1} = 2f_r - f_{r-1} + (\Delta\tau)^2 \left(f"_r + \frac{1}{12} \Delta^2 f"_{r-2}\right) \tag{A3}$$

With the approximate value of f_{r+1} given by equation (A3), an approximate value of $\Delta^2 f"_{r-1}$ may be found. Equation (A2) is then used to correct and check the approximate value of f_{r+1} found by equation (A3). The suggestion in reference 8 that the interval $\Delta\tau$ be chosen sufficently small so that there is little change in the values of f_{r+1} obtained from these two equations is followed in the present paper.

Initial Values

As bending of the column progresses, the strain in the convex flange eventually reaches a maximum and reverses. When reversal occurs, it is necessary to change the stress-strain relation for the convex flange which unloads elastically. Changing the stress-strain relation alters the form of $g(f,\tau)$; thus, the problem may be considered as consisting

of two parts, (1) prereversal and (2) postreversal, both of which require three initial values in order to start the recurrence process.

Prereversal.- The required initial values for the prereversal phase can be determined by expanding the dimensionless lateral deflection in a Taylor's series about $\tau = 0$, subject to the assumed initial conditions (1). The ratios of the moduli E_{S_L}/E and E_{S_R}/E which appear in equation (21) are implicit functions of f and therefore differentiation of the equation is impractical. However, during the initial stage of loading the values of these ratios often may be assumed to be constant and equal to unity. Such an assumption permits differentiation of equation (21) in order that the higher-order derivatives involved in the Taylor's series may be found. The following relation obtained from the series expansion and the assumed initial conditions provides the required initial values of f:

$$f_n = e + \frac{e\Omega}{\left(\epsilon_E/\epsilon_1\right)^3}\frac{(n\,\Delta\tau)^3}{3!} - \frac{e\Omega^2(2 + e^2)}{2\left(\epsilon_E/\epsilon_1\right)^5}\frac{(n\,\Delta\tau)^5}{5!} + \cdots \qquad (A4)$$

For those stress-strain curves which have a small, or no, elastic region (for example, $n = 2$ in the Ramberg-Osgood stress-strain curve representation), the assumption that the ratios of the moduli are unity is, of course, not valid. Nevertheless, the initial values of f obtained from equation (A4) may be used as the first trial values for an iteration procedure. An iteration expression can be derived by assuming that a second-degree parabola is sufficiently accurate to describe f'' in the neighborhood of $\tau = 0$. Integration of the parabola yields the following expression for f in terms of f'':

$$f_n = \frac{n^3}{24}\left[(n - 2)f''_2 + 2(4 - n)f''_1 + \left(n - 6 + \frac{12}{n}\right)f''_0\right](\Delta\tau)^2 + nf'_0\,\Delta\tau + f_0$$

$$(n = 0, 1, 2) \qquad (A5)$$

The trial values of f obtained from the series expansion are substituted into equation (A1) to find the corresponding trial values of f'', which are then substituted into equation (A5) to yield better values of f. The procedure is repeated until the values of f converge.

Postreversal.- As was previously mentioned, the integration process must be started anew at the point where strain reversal occurs. The

values of f, f', and f'' at τ_{rev} must be determined for they are used as initial conditions for the new integration problem. Strain reversal will generally occur at some value of τ which is not a multiple of $\Delta\tau$, and, therefore, the point at which reversal occurs must be located numerically or graphically. The required initial values of f and f'' are found by the following procedure:

1. Find $\left(\epsilon_R/\epsilon_1\right)_{max}$ and τ_{rev} numerically or graphically from plots of ϵ_R/ϵ_1 against τ.

2. Solve for f_{rev} by using equation (16b).

3. By using the known value of f_{rev}, solve equation (A1) for f''_{rev}.

Inasmuch as the velocity f' of lateral deflection does not appear in the solution, it is more difficult to find f'_{rev}. An approximation to f'_{rev} can be obtained as follows:

$$f'_{rev} = f'_a + \int_{\tau=a}^{\tau=\tau_{rev}} f''d\tau \tag{A6}$$

where a is some value of τ in the prereversal phase of the problem. By assuming that

$$f' \approx \frac{\Delta f}{\Delta\tau} \tag{A7}$$

equation (A6) can be written as

$$(\Delta\tau)f'_{rev} = (\Delta f)_a + \Delta\tau \int_{\tau=a}^{\tau=\tau_{rev}} f''d\tau \tag{A8}$$

The first differences Δf which are used in the solution are plotted at the midpoints of the intervals. The quantity $(\Delta\tau)f'_{rev}$ is evaluated by numerically integrating the f'' values between the last midinterval point before reversal ($\tau = a$) and τ_{rev}, and adding the result to the value of Δf at that last midinterval point. In the present case,

the error involved in the first-order approximation, equation (A7), is small, and the use of the approximation is therefore justified. The errors in the term $(\Delta\tau)f'_{rev}$ and the values of f calculated from equation (A5) are, of course, much smaller than the error in equation (A7).

In addition to the initial conditions, two additional sets of f and f'' are required to restart the integration. These are obtained by using equation (A5) and the associated iteration procedure. The first trial values in this case are obtained by interpolating the pre-reversal solution, which was extended a few increments in τ beyond the point at which reversal occurred.

Interval of Argument

In the present paper the interval $\Delta\tau$ has been selected to provide a minimum of 10 intervals per period of the first natural frequency in transverse bending. For the faster loading rates, in which cases there is only a fraction of a period of oscillation before the maximum load is reached or before the strains become prohibitively large, as many as 600 intervals per period of natural frequency were used.

REFERENCES

1. Shanley, F. R.: Inelastic Column Theory. Jour. Aero. Sci., vol. 14, no. 5, May 1947, pp. 261-267.

2. Duberg, John E., and Wilder, Thomas W., III: Inelastic Column Behavior. NACA Rep. 1072, 1952. (Supersedes NACA TN 2267.)

3. Wilder, Thomas W., III, Brooks, William A., Jr., and Mathauser, Eldon E.: The Effect of Initial Curvature on the Strength of an Inelastic Column. NACA TN 2872, 1953.

4. Hoff, N. J.: The Process of the Buckling of Elastic Columns. PIBAL Rep. No. 163 (Contract No. N6onr-26308), Dec. 1949.

5. Hoff, N. J., Nardo, S. V., and Erickson, Burton: The Maximum Load Supported by an Elastic Column in a Rapid Compression Test. PIBAL Rep. No. 185 (Contract No. N6onr-26308; Project No. NR 064-298), Mar. 1951.

6. Chawla, J. P.: Numerical Analysis of the Process of Buckling of Elastic and Inelastic Columns. PIBAL Rep. No. 175 (Contract No. N6onr-26308; Project No. 064-298), Sept. 1950.

7. Ramberg, Walter, and Osgood, William R.: Description of Stress-Strain Curves by Three Parameters. NACA TN 902, 1943.

8. Levy, H., and Baggott, E. A.: Numerical Solutions of Differential Equations. First Am. ed., Dover Pub., Inc., 1950, pp. 154-157.

TABLE 1.- CASES OF DYNAMIC COLUMN BUCKLING

FOR WHICH SOLUTIONS WERE OBTAINED

Case	n	σ_T/σ_1	ϵ_E/ϵ_1	e	Ω	$\Delta\xi$
1	10	1.0	5.2857	0.01	1	0.05
2	10	1.0	5.2857	.01	10	.05
3	10	1.0	5.2857	.01	10^2	.05
4	10	1.0	5.2857	.01	10^3	.01
5	10	1.0	5.2857	.01	10^4	.025
6	10	1.0	5.2857	.01	10^6	.003
7	10	1.0	5.2857	.00001	10^4	.025
8	10	1.0	5.2857	.0001	10^4	.025
9	10	1.0	5.2857	.001	10^4	.025
10	10	1.1	12.2160	.01	10^4	.05
11	10	.9	2.3943	.01	10^4	.01
12	10	.8	1.2602	.01	10^4	.005
13	10	.7	.8211	.01	10^4	.005
14	2	1.0	1.8571	.01	10^2	.05
15	2	1.0	1.8571	.01	10^3	.025
16	2	1.0	1.8571	.01	10^4	.01
17	2	1.0	1.8571	.01	10^6	.0015

TABLE 2.- RANGE OF VELOCITIES EMPLOYED

[For velocity of compression-wave propagation $\sqrt{\frac{E}{m}} = 16{,}740$ ft/sec and $\frac{L}{\rho} = 58.6$]

Ω	Velocity	
	ft/sec	in./min (a)
1	8.14	5861.0
10	2.57	1855.0
10^2	.814	586.1
10^3	.257	185.5
10^4	.0814	58.61
10^5	.0257	18.55
10^6	.00814	5.861

[a]Maximum platen speed for commonly used hydraulic testing machines is approximately 5 in./min.

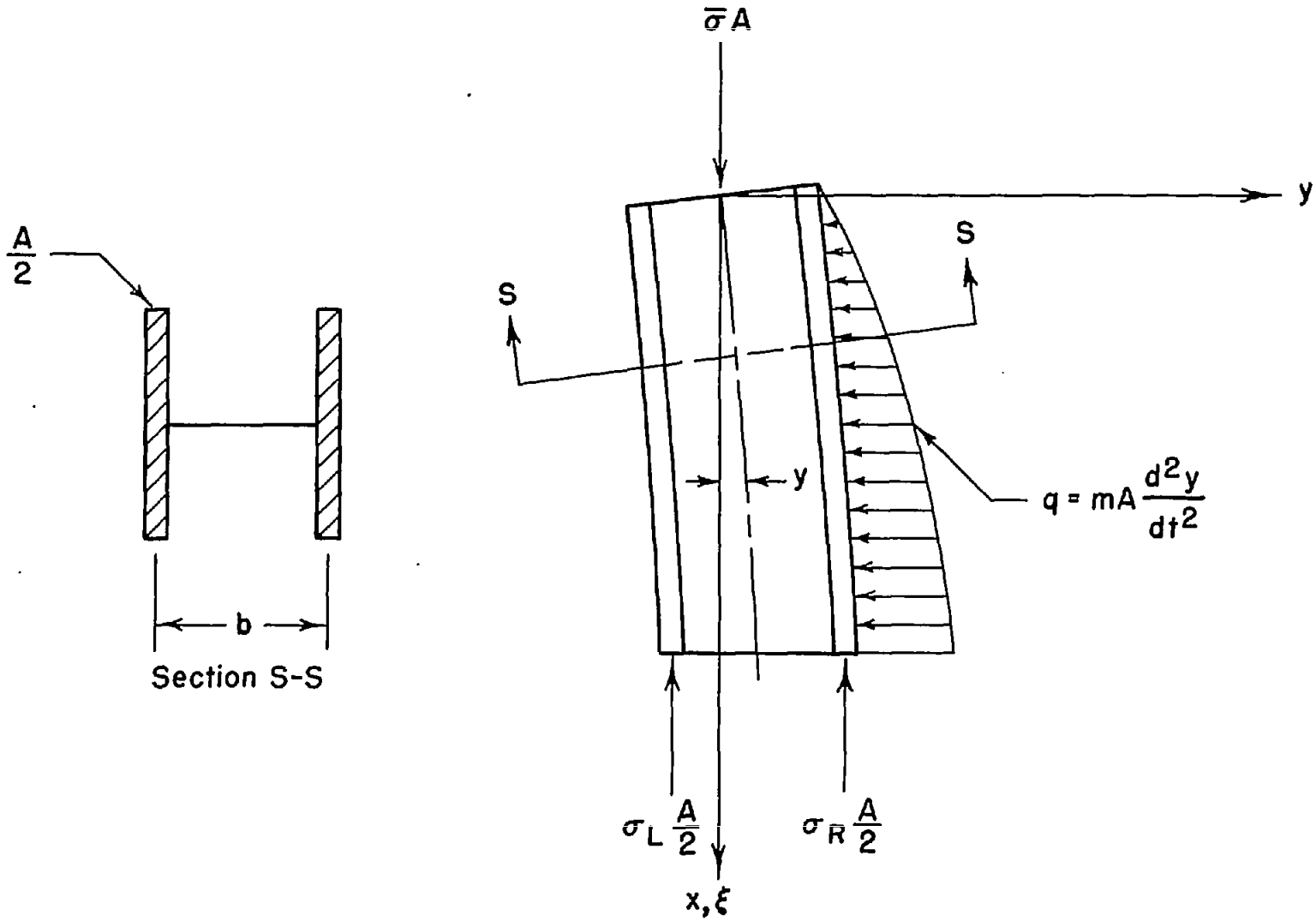

Figure 1.- Free-body diagram of an idealized H-section column.

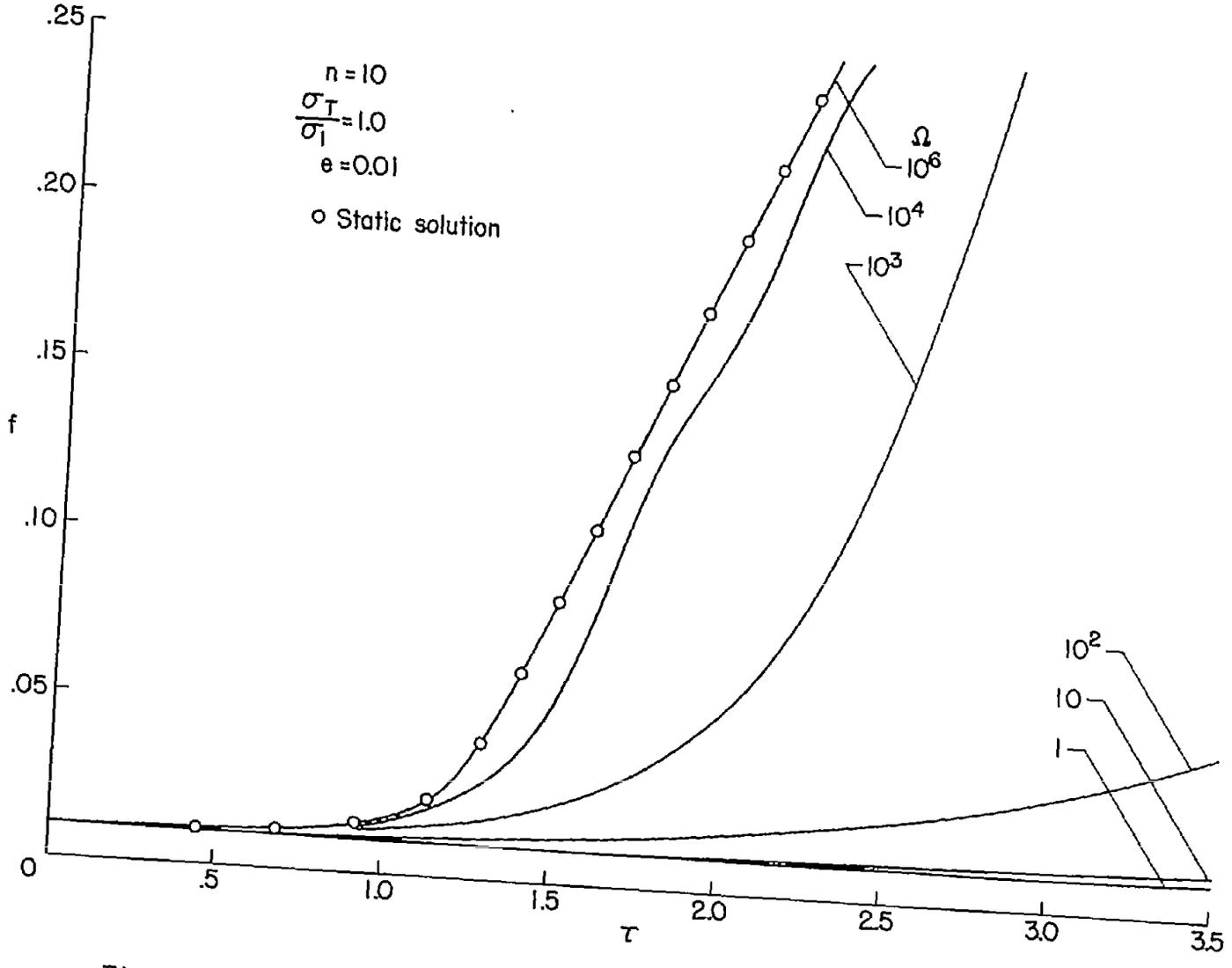

Figure 2.- Variation of lateral deflection with shortening for initially curved idealized H-section columns with various rates of end displacement.

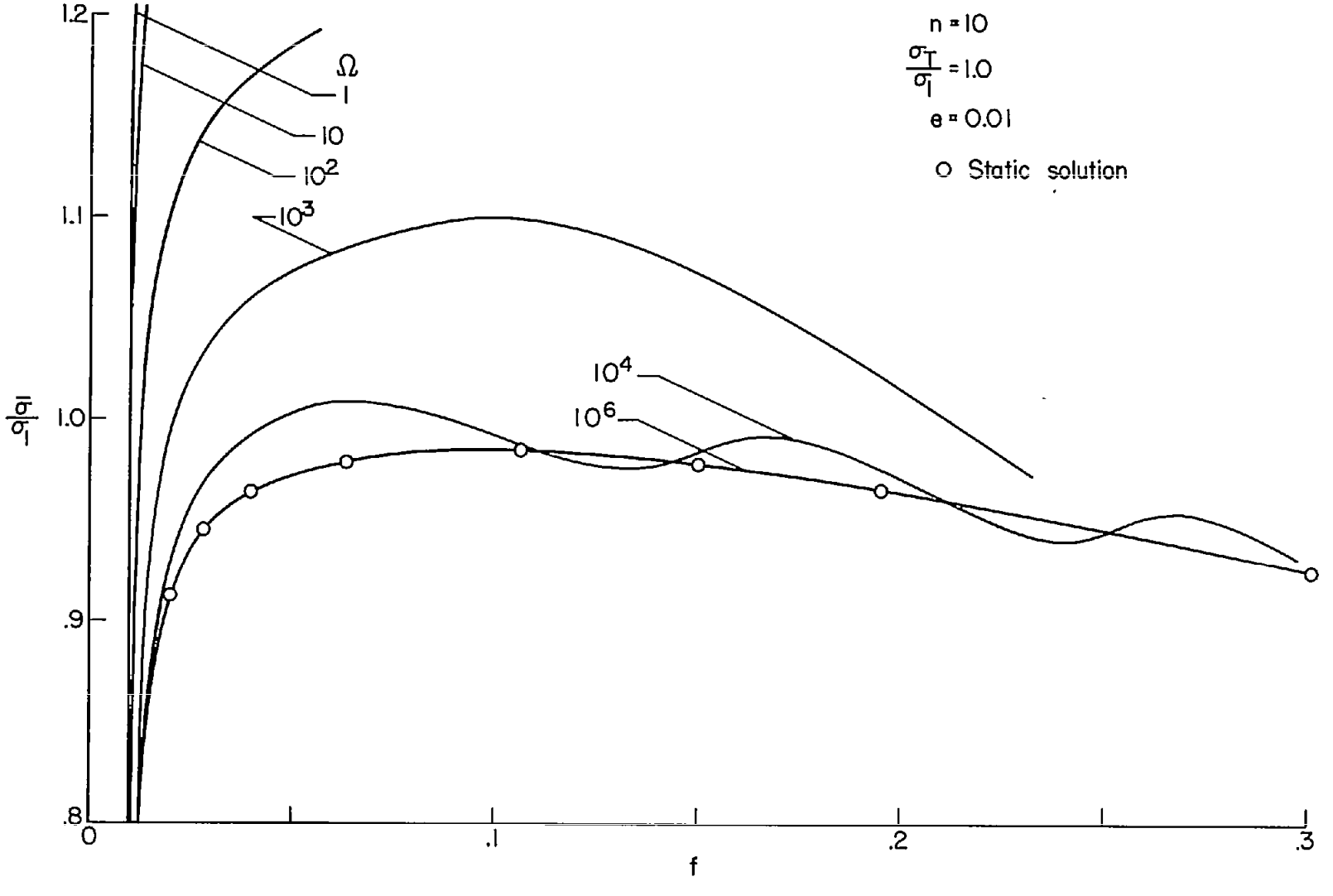

Figure 3.- Variation of load with lateral deflection for initially curved idealized H-section columns with various rates of end displacement. n = 10.

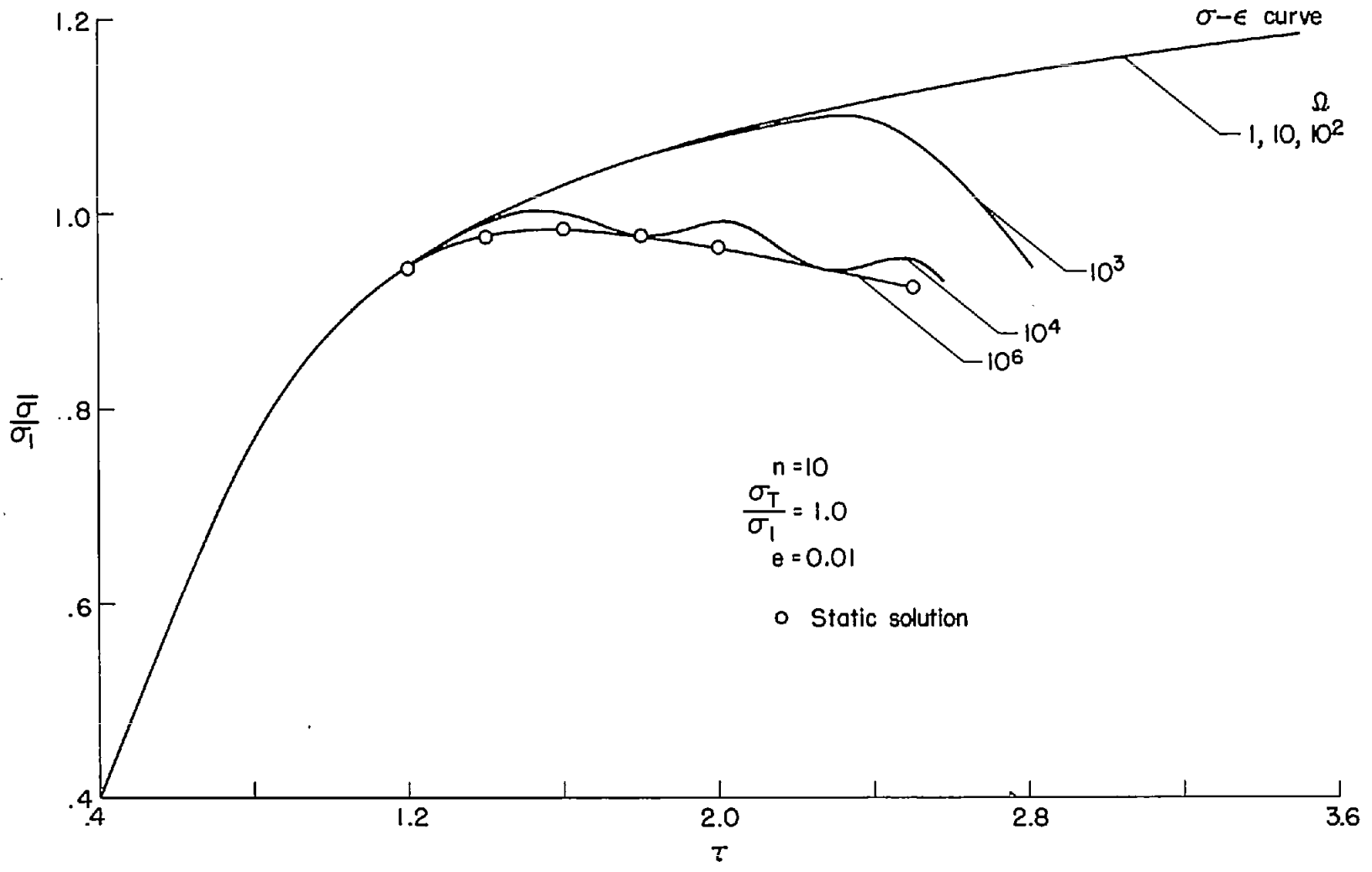

Figure 4.- Variation of load with shortening for initially curved idealized H-section columns with various rates of end displacement. n = 10.

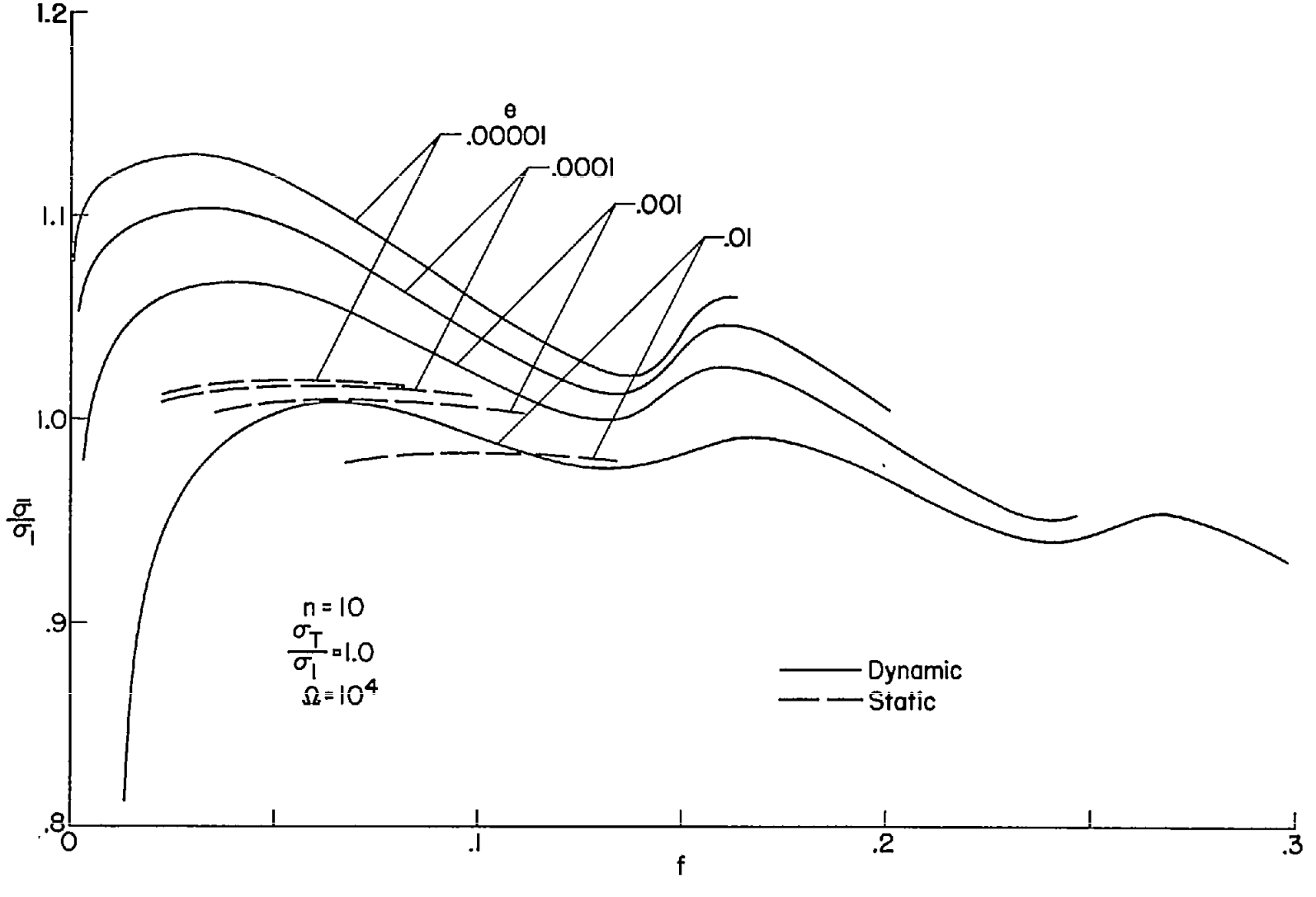

Figure 5.- Variation of load with lateral deflection for dynamically loaded idealized H-section columns with various initial curvatures.

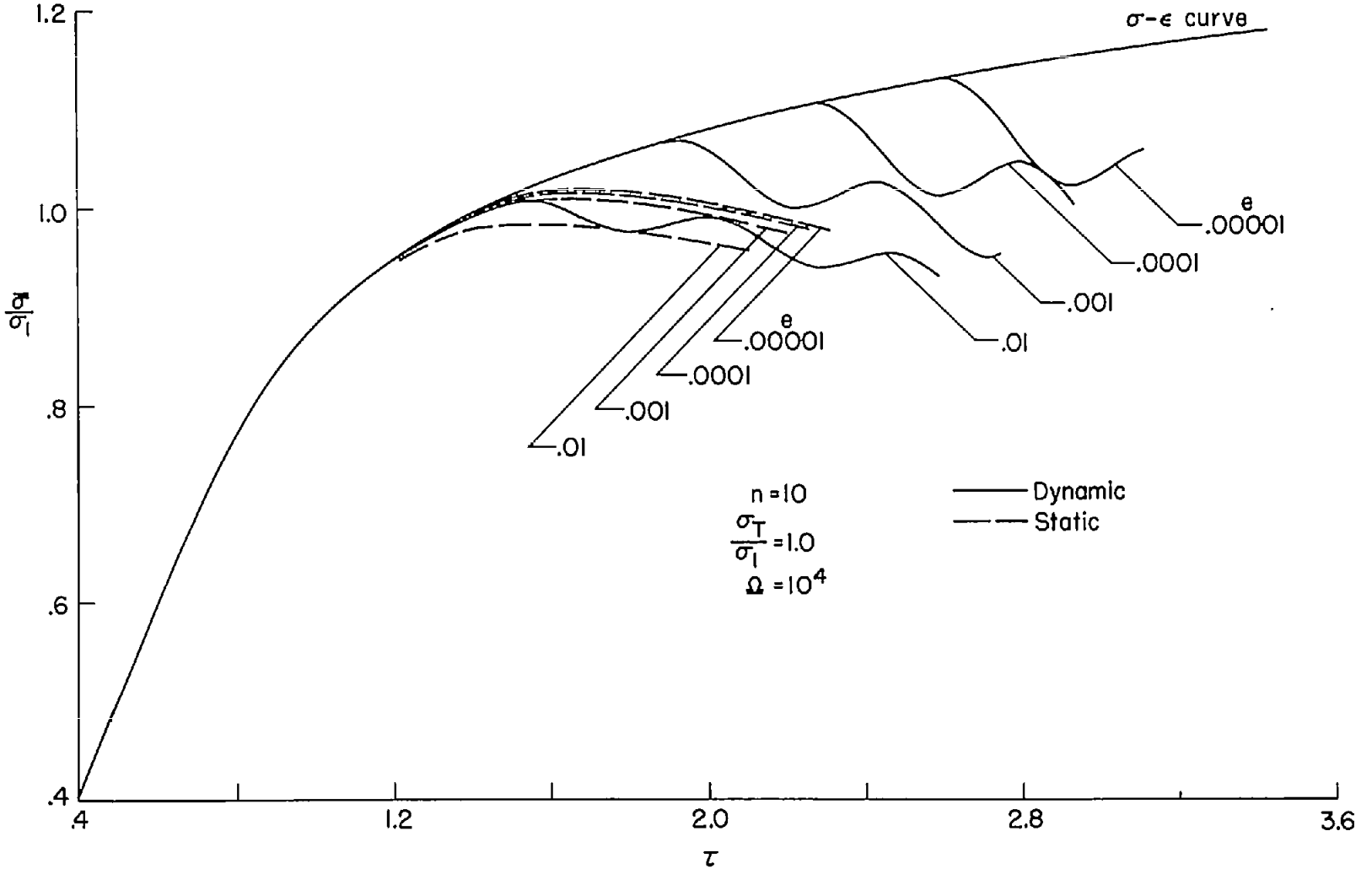

Figure 6.- Variation of load with shortening for dynamically loaded idealized H-section columns with various initial curvatures.

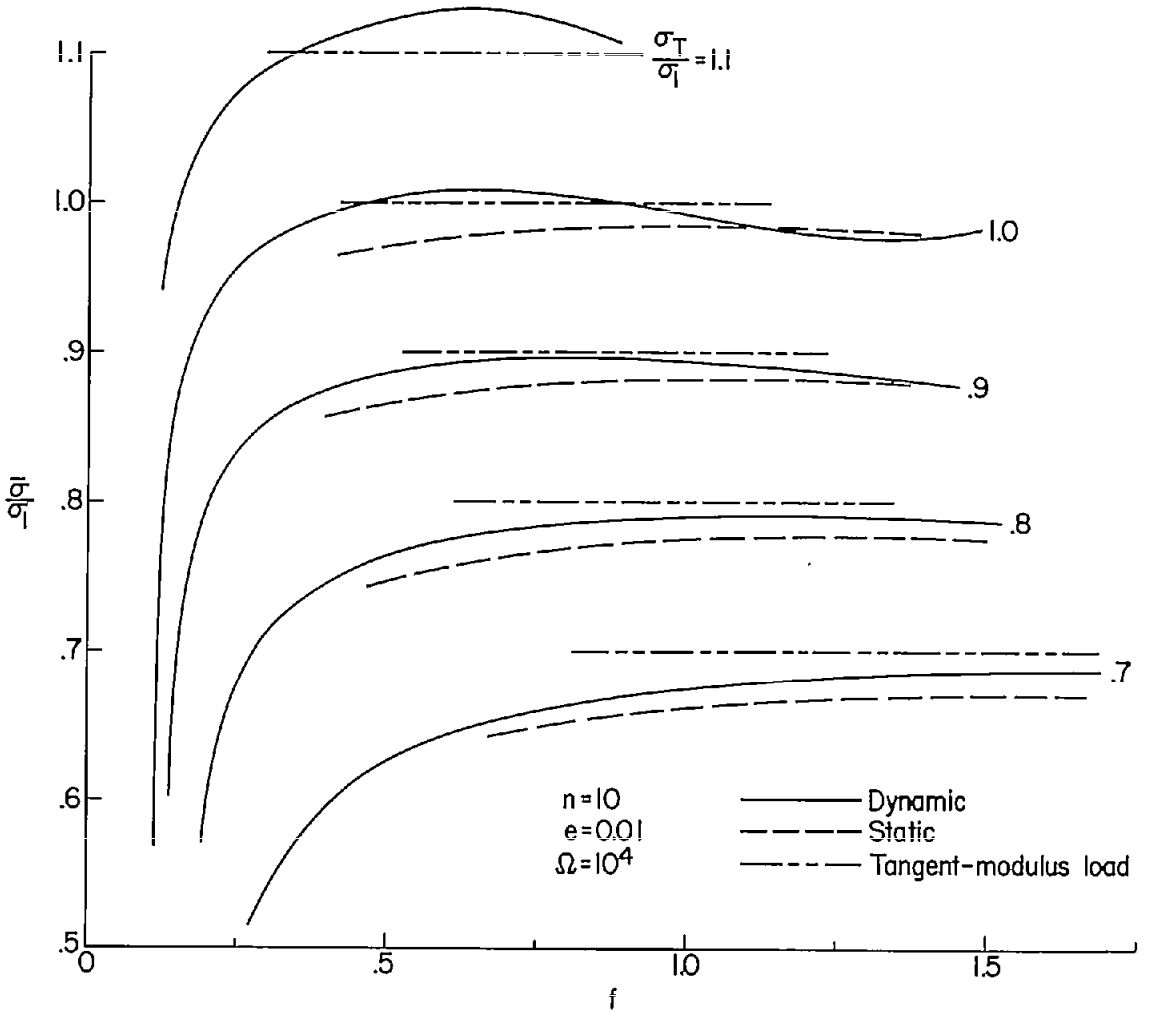

Figure 7.- Variation of load with lateral deflection for dynamically loaded, initially curved, idealized H-section columns of various lengths.

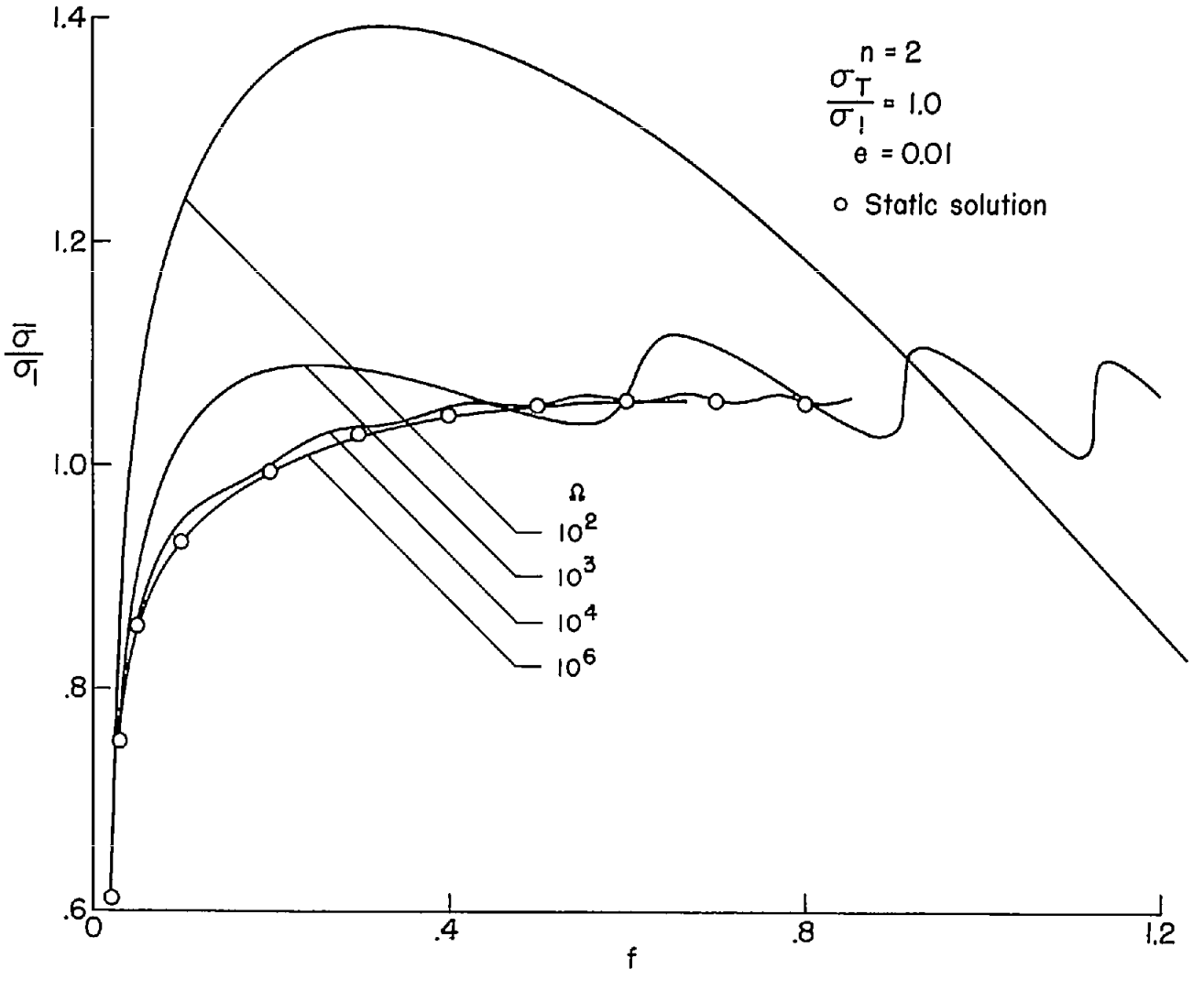

Figure 8.- Variation of load with lateral deflection for initially curved idealized H-section columns with various rates of end displacement. n = 2.

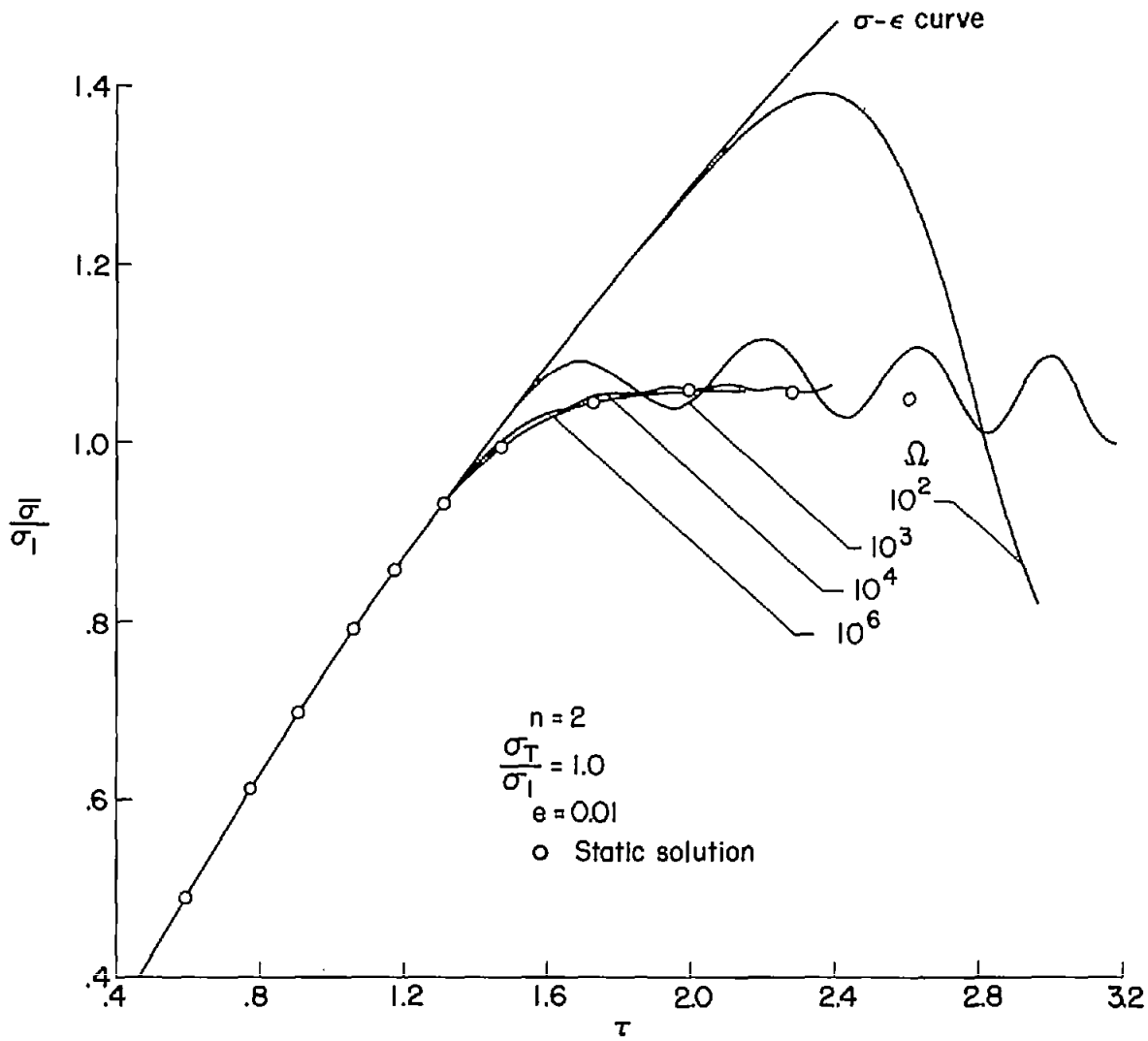

Figure 9.- Variation of load with shortening for initially curved idealized H-section columns with various rates of end displacement. n = 2.

NACA-Langley - 8-25-54 - 1000